

DESULFURIZATION KINETICS OF HIGH LEAD AND ZINC SULFIDE CONTAINING SLAG WITH OXYGEN BLOWING

K. Ouyang, Z.-H. Dou, T.-A. Zhang *, Y. Liu, L.-P. Niu

School of Metallurgy, Northeastern University, Shenyang, China

(Received 21 January 2019; accepted 07 April 2019)

Abstract

The desulfurization process of lead and zinc slag is an important smelting process to obtain lead and zinc. The aim of this paper is to study the desulfurization process of high lead and zinc sulfide containing slag with oxygen blowing. The predominance area diagrams of the Pb-Zn-Fe-S-O system ($Pb/(Fe+Pb+Zn)=0.176$, $Zn/(Fe+Pb+Zn)=0.56$) at various temperature were thermodynamically constructed. The physical properties, the chemical composition and the phase transformation of the desulfurization slag were investigated. The thermodynamic results indicated that lead, zinc, and iron can be oxidized to form high lead and zinc slag. The experimental results illustrated that the sulfur content in the oxidation slag can be reduced to less than 1% as temperature increased up to 1573 K. The XRD analysis of as-quenched slag shows the PbS and ZnS phase decreased, while zincite and spinel phase ($Zn_xFe_{3-x}O_{4+y}$) emerged and increased as the reaction time increased. The desulfurization process of molten slag were considered to be the first-order reaction and the apparent activation energy was estimated to be 44.46 kJ/mol. Under the experimental conditions, the mass transfer in the gas and liquid phase was likely to be the restrictive step.

Keywords: Lead and zinc mixed ore; High lead-zinc sulfur slag; Desulfurization; Kinetics

1. Introduction

At present, the main raw material for lead smelting process to produce lead is lead sulfide concentrate. However, with the rapid consumption of high grade lead resources, complex refractory lead-zinc mixed ores with huge reserves have become an alternative choice for the lead production in China [1]. Among the bath melting processes, the oxygen-enriched smelting process for the extraction of lead from the lead sulfide concentrate is widely applied in the industrial production. It consists of oxidation and reduction process [2-5]. The oxygen-rich smelting process has strict requirements on the zinc content in raw materials, and the current oxidation process conditions could not deal with high-zinc raw materials ($Pb \leq 35$, $Zn \geq 15\%$). According to the predominance area diagrams of Pb-S-O system, Schuhmann et al [6] indicated that a successful lead bath smelting process could be reached when oxygen activity and temperature were accurately controlled. During the oxygen-enriched smelting process of lead and zinc bulk concentrate, high lead-zinc sulfur slag is formed after the lead and zinc bulk concentrate added to the melt. A series of complex chemical reactions and multiphase mass transfer are

carried out between the slag and oxygen, when oxygen is injected into the slag [7]. The lead, zinc and iron sulfide are oxidized to oxides and react with flux to form the high lead and zinc slag, followed by reduction process to produce crude lead and zinc. As described by Jahanshahi and Wright [8] in the reduction process of lead oxide, the reduction kinetics strongly depended on the slag chemistry, its oxidation state, partial pressure of CO in the reaction gas mixture, and temperature. They also pointed out that mass transfer in the gas phase was not the rate-limiting step in the reduction process. The smelting slag with high content of zinc unavoidably has a change to the slag physicochemical properties, which lead to a great influence on the mass transfer and reaction rate in the oxygen-enriched smelting process. The kinetics process is important to the desulfurization process of the molten high lead and zinc sulfide containing slag. Through the kinetics study of desulfurization process, the restrictive steps can be found to improve the technological parameter, and finally increase the smelting efficiency. However, literature on the kinetics of oxidation reactions involving high lead and zinc sulfide containing slag are limited and most studies focus on the reduction process.

*Corresponding author: zta2000@163.net



The aim of this paper is to reveal the molten slag desulfurization process and mechanism. The thermodynamic analysis of oxidation process of lead-zinc sulfur slag using O_2 was carried out. The effects of the temperature and O_2 flow on the desulfurization process were studied. Simultaneously, the behavior of slag phase in the process of oxidation and physicochemical property of slag were discussed as well.

2. Experimental

2.1 Sample preparation

The experimental material was lead-zinc bulk concentrates provided by a mining company in China, and the composition is presented in Table 1. It can be seen that the content of Pb and Zn in the lead-zinc bulk concentrates is 24.56% and 28.5%, respectively. The initial high lead and zinc sulfide containing slag used in the experiments was synthesized with the analytical grade PbO, ZnO, SiO_2 , FeO, CaO, and lead-zinc bulk concentrates. The FeO was produced by mixing chemically pure iron powder (Fe) and hematite (Fe_2O_3). The major difficulty for the experimental procedure is the high vapor pressure of lead sulfide at high temperature [9]. In order to prevent the volatilization of PbS during the heating process, the pure chemical reagent of PbO, ZnO, SiO_2 , FeO, and CaO was added to the crucible and melted to form slag at first, and then lead-zinc bulk concentrates were pressed into a cylinder (diameter: 15 mm; length: 10 mm; pressing pressure: 2.0 MPa). When the slag reached the experimental temperature, the cylinder was added to the melts.

2.2 Apparatus and procedure

Fig. 1 shows the schematic diagram of experimental device for the current work. The experimental device consisted of gas blown system, resistance furnace, and outlet gas treatment system. Alumina crucible was put in the high temperature atmosphere furnace with $MoSi_2$ heating elements. The experimental temperature was controlled by computer program and measured by Pt-13 pct Rh/Pt thermocouples at the base of the alumina crucible. The Al_2O_3 nozzle of 5 mm i.d was placed above about 5mm from bottom of crucible, through which O_2 gas was blown into the slag. In addition, calibrated flow meter was used to control the oxygen flow rate, and

the outlet oxygen pressure was 0.2 MPa. Furthermore, the alumina crucible was connected to an electronic balance by a high temperature alloy wire.

The experimental steps are as follow: The alumina crucible (inner diameter: 38 mm; height: 120 mm) containing 82.5 g of analytical grade PbO, ZnO, SiO_2 , FeO, and CaO mixture was put into a vertical tube furnace. The furnace was then heated to the required temperature at a heating rate of 8 K/min. When the experimental temperature was reached and equilibrated for 30min, the cylinder of lead-zinc bulk concentrates (weight: 67.5g) were added to the melts to form high lead and zinc sulfide containing slag. High lead and zinc sulfide containing slag was equilibrated at the experimental temperature for 3 to 5 min. After that, the molten slag started desulfurizing by impinging O_2 gas to the slag surface. At each experiment time point, the slag weight was measured through electronic balance above the furnace, and, in addition, a small amount of molten slag was removed by iron rod and quenched in water to analyze the sulfur content and structure of slag. The slag phase was analyzed by X-ray diffractometer (Bruker, D8 ADVANCE, Germany) and SEM-EDS (Hitachi, SU-8010, Japan). In addition, the sulfur content of experimental slag was analyzed by carbon and sulfur analyzer (AXS, G4, Germany).

The produced sulfur dioxide gas was absorbed by aqueous solution of hydrogen peroxide. In order to maintain the atmosphere of alumina tube, Ar was introduced into the furnace through the bottom gas inlet of the furnace at a constant gas flow rate of 600 mL/min.

Sulfur removal during the molten high lead-zinc sulfur slag's desulfurization process was defined by Eq. (1)

$$m_{S,tot} = m_{S,initial} - m_{Slag} \times W_S \quad (1)$$

Where $m_{S,tot}$ is the sulfur removal, g; $m_{S,initial}$ is the initial sulfur content of slag, g; W_S is the sulfur content of molten slag during desulfurization process, wt pct; m_{Slag} is the weight of molten slag during desulfurization process, g.

3. Results

3.1 Thermodynamics analysis

The predominance area diagrams for Pb-Zn-Fe-S-O system ($Pb/(Fe+Pb+Zn)=0.176$, $Zn/(Fe+Pb+Zn)=0.56$)

Table 1. Chemical composition of experimental material (wt. %)

Experimental material	Pb	Zn	Cu	S	SiO_2	TFe	CaO	Others
Lead-zinc bulk concentrate	24.56	28.5	2.56	28	4.38	10.08	0.08	1.84
High lead and zinc sulfide containing slag	25	25	1.15	12.6	13.04	10.17	6.5	6.54



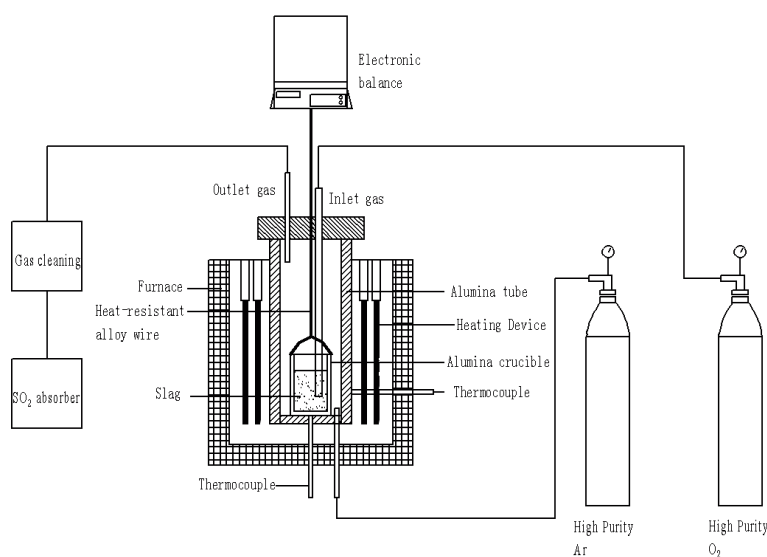


Figure 1. Diagram of experimental apparatus

at different temperatures was calculated by Factsage™ 6.4. As shown in Fig. 2, it can be seen that the stable region of $PbO(l)+ZnO(s)+ZnFe_2O_4(s)$ existed when oxygen and sulfur dioxide partial pressure was low. With the decrease of system temperature, the thermodynamic stability region of $PbO(l)+ZnO(s)+ZnFe_2O_4(s)$ was enlarged in the direction of Po_2 value. Region A was the coexistence region of lead oxide, zinc oxide, and iron oxide at temperature between 1473 and 1623 K. If the value of and were kept in region A, the lead, zinc, and iron could be oxidized to lead-zinc-iron oxide and react with flux to form high lead and zinc slag.

3.2 Desulfurization Process of Molten Slag with O_2 gas

Table 2 presents the composition of obtained oxidized slag at different experimental temperature with O_2 flow rate at 60 L/h. It can be seen that the slag composition has changed due to the volatilization of lead species during the experiment.

The results obtained from the desulfurization of the high lead and zinc sulfide containing slags (slag weight: 150 g) using 60 L/h of O_2 gas at different temperature are shown in Figure 3(a)-(b). Fig. 3(a) shows that the increase in temperature was conducive to the decrease of sulfur content in the slag. Moreover, the sulfur content of slag could be reduced to less than 1.5 wt. % after a period of 10 min. As seen in Fig. 3(b), the experimental temperature had a great influence on the weight of the slag, and the weight of the slag was decreased to about 115g when the reaction temperature was at 1623 K. However, as shown in Fig. 3(a) and (b), in the desulfurization period from 0 to 4 min, both weight and sulfur content of slag decreased dramatically, which indicated that in

the initial desulfurization stage the volatilization rate of lead species was very high. In order to eliminate the impact of high temperature volatilization of lead species on experimental results, the sulfur content and weight of molten slag were adjusted by a series of comparative experiments with Ar flow rate of 60 L/h at each experimental temperature. And the actual sulfur removed was revised according to the Eq. (2).

$$m_{S, \text{Revise}} = m_{S, \text{tot}} - m_{S, \text{Ar}} \quad (2)$$

Where $m_{S, \text{Revise}}$ is the revised sulfur removed, g; $m_{S, \text{Ar}}$ is the sulfur removed of molten slag with Ar flow rate of 60 L/h at each experimental temperature, g;

Fig. 4 and 5 show the revised results obtained according to Eq. (2). As is shown in Fig. 4, the experimental temperature played an important role in the desulfurization of the high lead-zinc sulfur slag. The higher the temperature, the higher amount of sulfur was removed. As the experimental temperature increased to 1573 K, the slag sulfur removal increased dramatically. The effect of oxygen flow rate on sulfur removal was studied as well, and the result is given in Fig. 5. It can be seen that the sulfur removal increased with the increase of oxygen flow rate. Thus, increasing temperature and oxygen flow rate is beneficial to accelerate the desulfurization reaction.

Table 2. Chemical composition of the oxidized slag at various temperature (wt. %)

Temperature/ K	Pb	Zn	Cu	S	SiO ₂	TFe	CaO
1473	22	27.5	1.18	1.5	15.4	12.19	7.4
1523	20.8	28.5	1.21	1	15.04	12	7.71
1573	17.1	30.8	1.22	0.7	15.46	12.58	7.53
1623	14.8	31.2	1.34	0.21	16.02	13.1	8.12



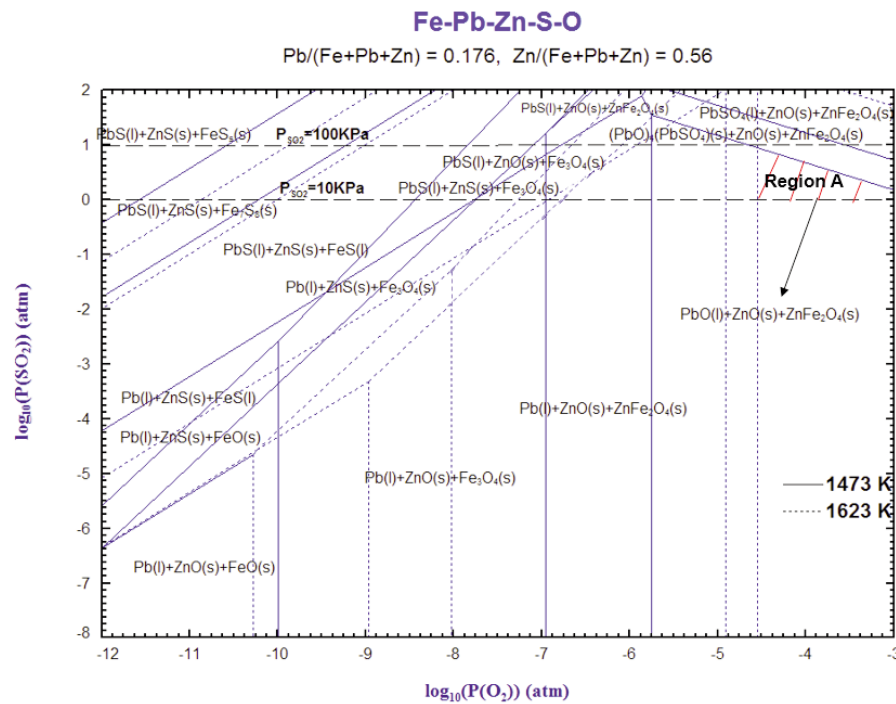


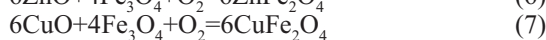
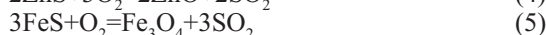
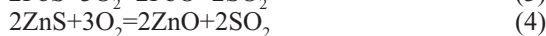
Figure 2. Predominance area diagrams of the Pb-Zn-Fe-S-O system (Pb/(Fe+Pb+Zn)=0.176, Zn/(Fe+Pb+Zn)=0.56) at 1473-1623 K

3.3 Molten Slag Behaviors

The phase changes of the quenched slag under different desulfurization period are shown in Fig. 6. It can be seen that the initial phases for the slag were identified as PbS and ZnS. With the reaction time increasing to 3 min, the diffraction peaks for metal lead became observable, whereas the peak intensity for ZnS decreased substantially. As the reaction time continued to increase, the zincite (ZnO) and spinel phase ($Zn_xFe_{3-x}O_{4+y}$), such as $ZnFe_2O_4$, emerged and the lead related peaks vanished. At the reaction time of 10 min, the zincite and spinel phase became the main phase of precipitation in slag, and the diffraction peaks for PbS and ZnS finally disappeared. Fig. 7 shows the SEM-EDS image of obtained oxidized slag, which was further confirmed through the observation by XRD.

4. Discussion

The main reactions of slag desulfurization by oxygen are as follows:



The whole experimental process was carried out in the constant temperature zone (temperature variation:

± 2 K). As a result, it is assumed that the temperature change in the desulfurization process can be neglected. The desulfurization process of high lead and zinc sulfide containing slag is a complex system. Therefore, the relationship between sulfur molar concentration in molten slag and reaction time was used to determine the reaction order ($n=0, 1$ and 2) of desulfurization reaction.

$$-\frac{dc_s}{dt} = kc_s^n \quad (8)$$

Where C_s is the sulfur molar concentration in slag, $\text{mol} \cdot \text{m}^{-3}$; t is the reaction time, s;

When the reaction is the zero-order reaction:

$$c_0 - c_s = kt \quad (9)$$

When the reaction is the first-order reaction:

$$\ln \frac{c_0}{c_s} = kt \quad (10)$$

When the reaction is the second-order reaction;

$$\frac{1}{c_s} - \frac{1}{c_0} = kt \quad (11)$$

Results of slag oxidation at 1573 K and at a constant O_2 flow of 60 L/h were brought into the above three equation for fitting, and the fitting results are shown in Fig. 8. When the reaction was of the first order, the correlation coefficient R^2 was estimated to 0.977, which was higher than the correlation coefficient



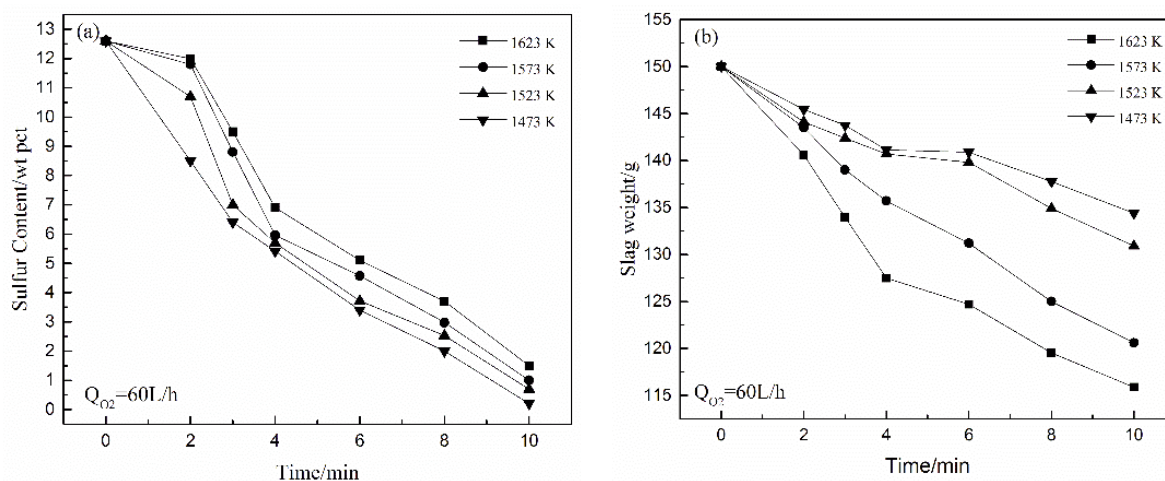


Figure 3. The variation of sulfur content and weight of slag with time during the desulfurization process

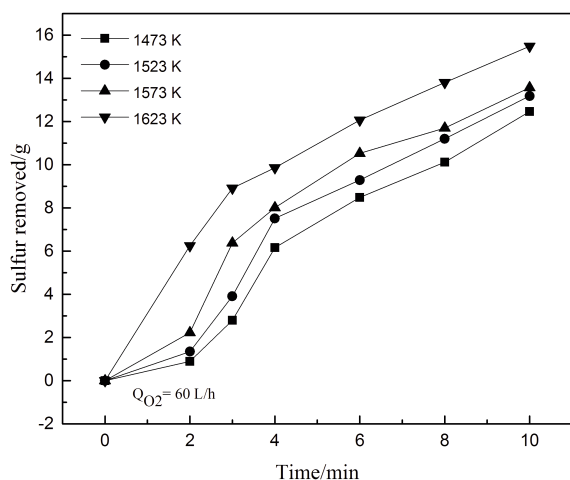


Figure 4. The relationship between sulfur removed and time at different temperatures

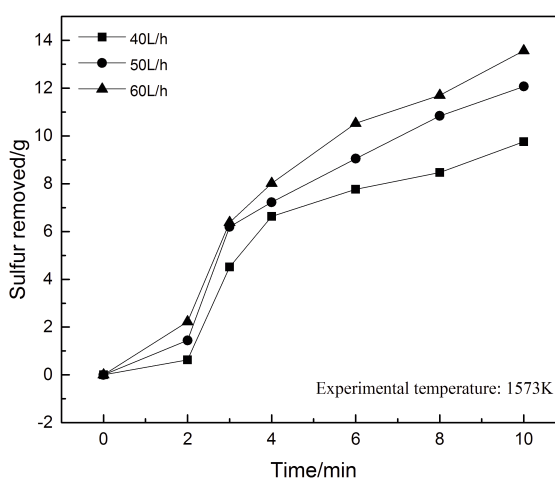


Figure 5. The relationship between sulfur removed and time at different oxygen flow rates

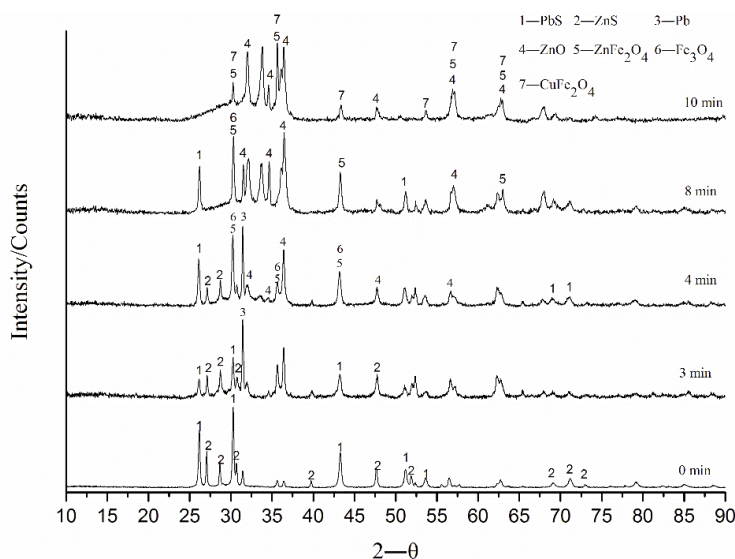


Figure 6. The relationship between XRD diffraction analysis of as-quenched slag and desulfurization time



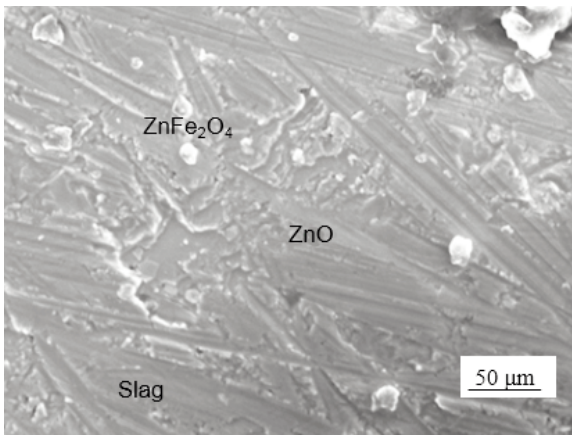


Figure 7. Morphology of obtained oxidized slag quenched at 1573 K

of the zero order and second order reactions. The results indicated that the molten slag desulfurization with oxygen gas was in accordance with a first-order reaction.

Fig. 9 shows the linear fitting of the natural logarithm of sulfur content of slag and time at experimental temperature from 1473 K to 1623 K, and the slope of fitting line was the reaction rate coefficient (K_d). The relation between $\ln K_d$ and time (t) is presented in Fig. 10. According to the linear fitting result, the apparent activation energy was estimated to be 44.46 kJ/mol. As a result, the results could be expressed by Eq. (12):

$$\ln k_{total} = -\frac{5347.6}{RT} + \ln k_0 \quad (12)$$

Where k_{total} is the reaction coefficient; and T is the experimental temperature, K.

Fig. 11 shows the schematic diagram of gas-slag

reaction model for desulfurization process. In this study, the double film theory can describe the reaction between molten slag and oxygen gas which is considered to be a typical gas-liquid reaction [10]. The gas-liquid reaction consists of the following five steps:

The small O_2 bubble was formed at the outlet of the nozzle, and grew to form a vapor phase boundary layer;

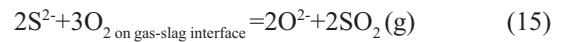
The oxygen diffused to the gas-slag reaction boundary layer:

$$(O_2)_{in\ bubble} = (O_2)_{on\ gas-slag\ interface} \quad (13)$$

The sulfur ions migrated to the gas-slag reaction boundary layer:

$$S^2_{slag} = S^2_{on\ gas-slag\ reaction\ boundary\ layer} \quad (14)$$

The gas bubbles reacted with sulfur ions at the gas-slag reaction boundary layer and generated oxygen ions:



The O^2 product diffused into the molten slag.

The chemical reaction rate should have the following relationship in terms of the first-order reaction:

$$\frac{1}{k_{total}} = \frac{1}{k_d} + \frac{1}{k_r} \quad (16)$$

Where k_d is the mass transfer coefficient, $m \cdot s^{-1}$; k_r is the chemical reaction rate constant, $m \cdot s^{-1}$.

The reaction between gas, high temperature melts, and gas transfer process, which correspond to step 1-2,

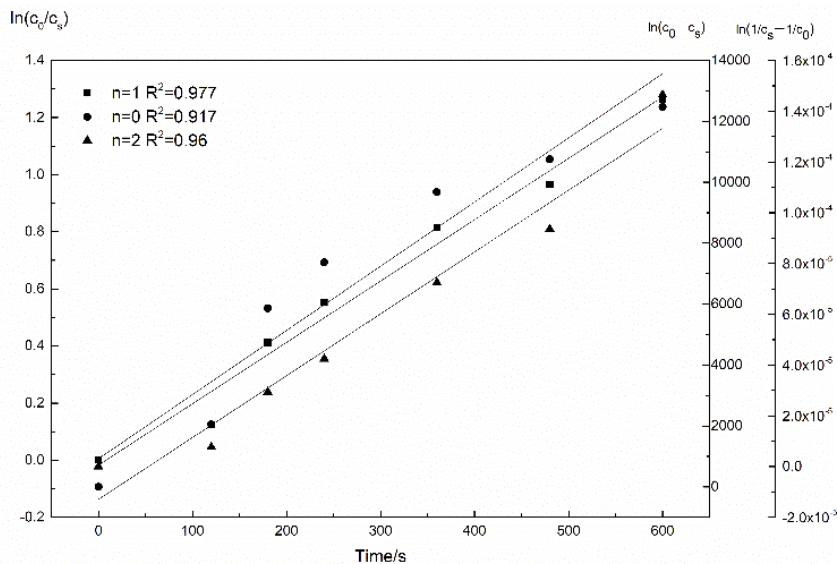


Figure 8. Estimation of reaction order



4, were considered to be very fast and it was not likely to become a limiting part of the reaction. So the mass transfer in gas and liquid phases is supposed to be the restricted step which corresponds to step 3 and step 5. Therefore, the desulfurization rate constant (k_{total}) could represent the mass transfer coefficient (k_d) of sulfur ions and oxygen ions in the slag during diffusion.

The penetration model which is based on the double film theory can depict the mass transfer process (Eq. 17). Oxygen migrates into the slag micro-element volume. After a period of time t , the volume leaves the interface, and then another volume element interacts with the phase, repeating the mass transfer process described above, and finally achieving mass transfer between the two phases. The applicable range of Eq. (17) could be determined by Fick similarity equation [11]:

$$\pi \leq \frac{L^2}{Dt_e} \leq \infty \quad J = 2\sqrt{\frac{D}{\pi t_e}}(C_i - C_b) \quad k_d = 2\sqrt{\frac{D}{\pi t_e}} \quad (17)$$

Where L is liquid film thickness, m (under the

experimental conditions, the film thickness could be considered as 120 μm [12]); D is the diffusion coefficient, $\text{m}^2 \cdot \text{s}^{-1}$; J is the diffusion mass flow, $\text{mol} \cdot \text{m}^{-2} \cdot \text{s}^{-1}$; C_i is the interface concentration of diffusion phase, $\text{mol} \cdot \text{m}^{-3}$; C_b is the concentration of diffusion liquid phase, $\text{mol} \cdot \text{m}^{-3}$; t_e is the average contact time of each micro-element in the fluid with the entire bubble, s.

In the desulfurization period of molten high lead-zinc sulfur slag, the oxygen gas injected by the nozzle was dispersed into tiny bubbles. During the floating process of the bubbles in the slag, the contact time of the liquid micro-element and the bubble from the head to the tail could be considered as the average contact time of micro-element, and expressed as follows [13]:

$$t_e = \frac{d}{v} \quad (18)$$

Where v is the bubble floating velocity, $\text{m} \cdot \text{s}^{-1}$; d is bubble diameter, m.

The oxygen flow rate was very low ($R_{e0} < 500$) in this study, and as a result, the size of generated

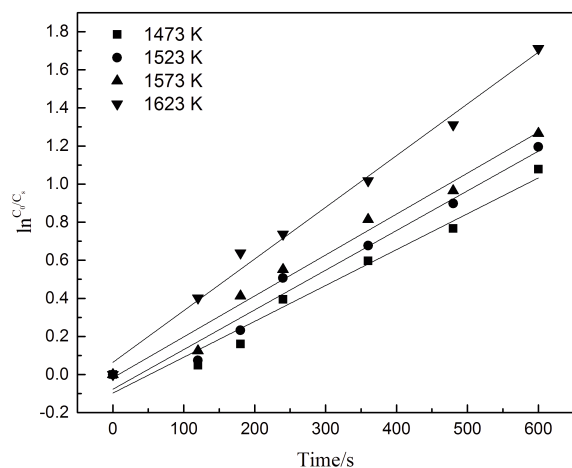


Figure 9. Calculation of reaction rate at different temperature

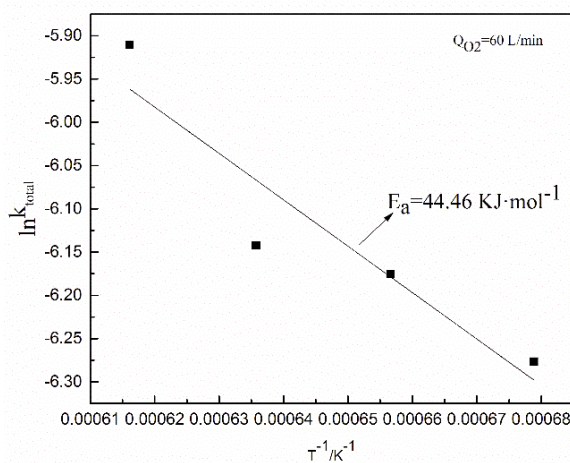


Figure 10. Relation between $\ln k_{total}$ and $1/T$

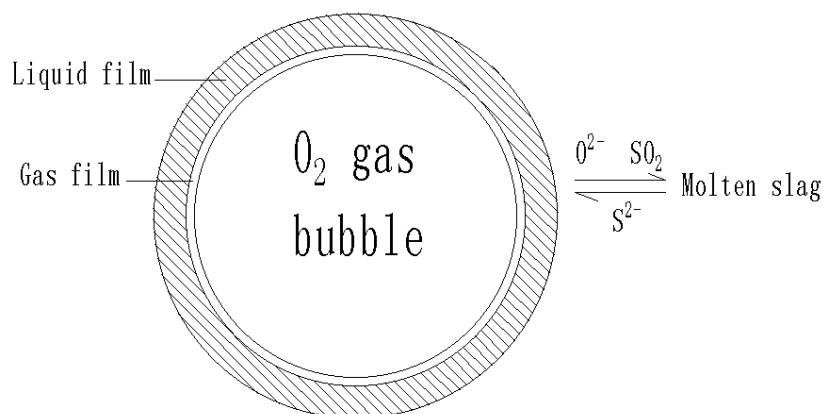


Figure 11. Schematic diagram of gas-slag reaction model for desulfurization process



bubble depended on the relationship between buoyancy and surface tension. When the buoyancy of the bubble exceeded the downward force due to surface tension, the bubble exited the nozzle. The bubble diameter could be calculated according to the following formula [10]:

$$\frac{\pi}{6}d_0^3(\rho_L - \rho_g)g = \pi d\gamma_s \quad (19)$$

Where d_0 is the bubble diameter, m; d is the nozzle diameter, m; γ_s is the slag surface tension, $\text{N}\cdot\text{m}^{-1}$; ρ_L is the slag density, $\text{kg}\cdot\text{m}^{-3}$; ρ_g is the gas density, $\text{kg}\cdot\text{m}^{-3}$; g is the gravity acceleration, $\text{m}\cdot\text{s}^{-2}$.

When Re is between 2 and 400, in addition, bubble diameter is less than 2 mm, the bubble could be regarded as a spherical bubble [10], and the floating velocity of bubbles can be obtained by Eq. (20):

$$v = \frac{d_0^2}{12\mu_L}(\rho_L - \rho_g)g \quad (20)$$

Where μ_L is the viscosity of slag, $\text{Pa}\cdot\text{S}$.

In this study, the cylinder contact method, standard Archimedes method, and rotating method was used to measure the surface tension, density, and viscosity of lead and zinc sulfide containing slag, respectively, and the results are listed in Table 3. As shown in Table 3, under the experimental condition, the value of L^2/Dt was within the range, indicating that the gas-liquid reaction mass transfer process could be treated with penetration model. According to the Eq. (17), shortening the time of replacing old bubbles with fresh bubbles on the interface was beneficial to the improvement of the mass transfer coefficient. As a result, this could accelerate the reaction rate. The rate and progress of the oxidative desulfurization reaction could be controlled through the change of reaction temperature and flow rate of the blowing gas.

In the process of oxidative desulfurization of molten high lead-zinc sulfide slag, it is often a multi-bubble dispersion system, and its total mass transfer and gas flow are closely related. According to the penetration model, the main parameters affecting the mass transfer in gas-slag during desulfurization process could be expressed by Eq. (21) in terms of similarity with equation [13].

$$Sh = f(Re, Sc, We), \quad Sh = m_1 \cdot Re^{m_2} \cdot Sc^{m_3} \cdot We^{m_4} \quad (21)$$

Table 3. D and L^2/Dt from 1473 to 1623 K

T/K	$\mu_L/\text{Pa}\cdot\text{S}$	$\rho_L/\text{kg}\cdot\text{m}^{-3}$	$\gamma_s/\text{N}\cdot\text{m}^{-1}$	d/m	t_g/s	$D/\text{m}^2\cdot\text{s}^{-1}$	L^2/Dt
1473	0.495	4200	0.4341	0.001975	0.011403	3.16×10^{-8}	39.9
1523	0.285	4120	0.3833	0.002195	0.007435	2.53×10^{-8}	76.7
1573	0.157	4040	0.2955	0.002791	0.005313	1.93×10^{-8}	140.6
1623	0.13	4003	0.267	0.003061	0.004869	2.81×10^{-8}	105.4

Where Sh is the Sherwood number; Re is the Reynolds number; Sc is the Schmidt number; We is the Weber number; m_1, m_2, m_3, m_4 are the constants, respectively. These similarity numbers can be expressed by Eq. (22):

$$Sh = \frac{k_d \times d}{D}, \quad Re = \frac{v_g \times d \times \rho_L}{u_L}, \quad (22)$$

$$Sc = \frac{u_L}{\rho_L \times D}, \quad We = \frac{\gamma_s}{\rho_L \times g \times d^2}$$

Where k_d is the total mass transfer coefficient, $\text{m}\cdot\text{s}^{-1}$; v_g is the O_2 gas outlet rate, $\text{m}\cdot\text{s}^{-1}$.

According to the parameters listed in Table 3, the value of $Sh, Re, Sc,$ and We were calculated under different experimental conditions. The calculated results were listed in Table 4. As a result, Eq. (23) could be obtained as following:

$$Sh = 0.112 \cdot Re^{0.985} \cdot Sc^{0.51} \cdot We^{0.137} \quad (23)$$

Therefore:

$$\frac{k_d \times d}{D} = 0.112 \times \left(\frac{v_g \times d \times \rho_L}{u_L} \right)^{0.985} \times \left(\frac{u_L}{\rho_L \times D} \right)^{0.51} \times \left(\frac{\gamma_s}{\rho_L \times g \times d^2} \right)^{0.137} \quad (24)$$

So:

$$k_d = 0.112 \times \frac{v_g^{0.985} D^{0.49} \rho_L^{0.338} \gamma_s^{0.137}}{u_L^{0.475} d^{0.289} g^{0.137}} \quad (25)$$

The reaction rate is expressed in Eq. (26)

$$-\frac{dC}{dt} = k_{d,overall} \times C \quad t=0, C=C_0 \quad (26)$$

Where C is the volume molar concentration of the slag at t moment, mol/L ; $k_{d,overall}$ is the reaction rate constant;

Table 4. Similarity Numbers at different temperature

T/K	Sh	Re	Sc	We
1473	117.52	14.25	3725.22	2.7
1523	180.42	26.97	2739.35	1.97
1573	310.95	61.05	2015.73	0.96
1623	295.2	80.12	1156.97	0.73



The above equation can be described as follows:

$$C = C_0 \times e^{-k_d, \text{ overall} \times t} \quad (27)$$

The desulfurization reaction degree is defined as follows:

$$R = (1 - e^{-k_d, \text{ overall} \times t}) \times 100 \quad (28)$$

Where R is the desulfurization reaction degree, wt pct.

According to Eq. (25), the Eq. (28) can be described as follows:

$$R = \left(1 - e^{-0.112 \times \frac{v_g^{0.985} D^{0.49} \rho_L^{0.338} \gamma_s^{0.137}}{u_L^{0.475} d^{0.289} g^{0.137}} \times t} \right) \times 100 \quad (29)$$

Fig. 12 shows the comparison diagram of model fitting curve and experimental results. The calculation results were compared with desulfurization experiment results in order to verify the accuracy of Eq. (28). Based on the above comparison, the results show that the model fitted well with the actual data.

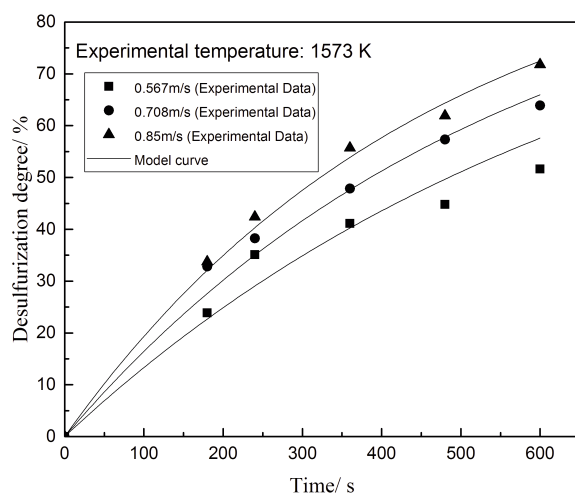


Figure 12 Comparison diagram of model fitting curve and experimental results for the desulfurization degree (experimental temperature: 1573 K)

5. Conclusions

In current study, the predominance area diagrams for the Pb-Zn-Fe-S-O system ($Pb/(Fe+Pb+Zn)=0.176$, $Zn/(Fe+Pb+Zn)=0.56$) at different temperatures were constructed. The thermodynamic analysis shows that lead and zinc could be oxidized to form the high lead and zinc slag.

The experiments results illustrated that the desulfurization rate of slag increased significantly and the sulfur content in the oxidation slag was below 1% as temperature increased up to 1573 K. The kinetics analysis indicated that the desulfurization rates of the

molten high lead and zinc sulfide containing slag were considered to be in the first-order reaction concerning sulfur content at temperatures between 1473 and 1623 K, with the apparent activation energy equivalent to 46.6 kJ/mol, and the mass transfer in gas and liquid phase is most likely to be the rate-controlling step under the experimental conditions. The XRD patterns of oxidation slag demonstrated that the sulfide phase decreased gradually, while the zincite and spinel phase emerged and increased as the reaction time increased. The mathematical model of total mass transfer coefficient (k_d) in gas-liquid reaction process was proposed and verified by experimental data, and the calculated results were consistent with the experimental data.

Acknowledgements

This study was supported by the National Natural Science Foundation of China (51674074, 51774078) and the Fundamental Research Funds for the Central Universities (N162505002).

References

- [1] Z.B. Yu, S. Zou, S.J. Liu, H.L. Luo, E.X. Zhang, Ming R&D, 35(4) (2015) 24-27 (in Chinese).
- [2] Z.T. Zhang, W.F. Li, J. Zhan, J. Min. Metall. Sect. B-Metall., 54 (2) B (2018) 179-184.
- [3] L. Chen, T. Yang, S. Bin, W. Liu, D. Zhang, W. Bin, L. Zhang, JOM, 66(9) (2014) 1664-1669.
- [4] Y. Zhang, T.R. Meadowcroft, Can. Metall. Quart., 43(3) (2004) 395-405.
- [5] Z.T. Zhang, X. Dai, W.H. Zhang, JOM, 69(12) (2017) 2671-2676.
- [6] R. Schuhmann, Jr., Pei-Chen Chen, P. Palanisamy, Metall. Mater. Trans. B, 7B (1976) 95-101.
- [7] Q.M. Wang, X.Y. Guo, Q.H. Tian, Trans. Nonferrous Met. Soc. China, 27 (2017) 946-953.
- [8] S. Jahanshahi, S. Wright, Metall. Mater. Trans. B, 48B (2017) 2057-2066.
- [9] S. Jin-hui, Hunan Nonferrous Metals, 20 (2004) 21-23 (in Chinese).
- [10] M. Fan-ming, Metallurgical Macrokinetics Basis, Metallurgical Industry Press, Beijing, 2014, p. 104 (in Chinese).
- [11] L.N. Zhang, L. Zhang, M.Y. Wang, Z.T. Sui, Trans. Nonferrous Met. Soc. China, 15(4) (2005), 938-943.
- [12] T. El. Gammal, E.A.T. Wosch, and H.T. Schriener, Proceedings of the 11th International Symposium on Molten Salts, San Diego, America, 1998, p. 429-434.
- [13] Z. Huai-wei, S. Xiao-yan, Z. Bo, H. Xin, Metall. Mater. Trans. B, 45B (2014) 582-589.



KINETIKA DESULFURIZACIJE ŠLJAKE SA VISOKIM SADRŽAJEM SULFIDA OLOVA I CINKA POSTUPKOM UDUVAVANJA KISEONIKA

K. Ouyang, Z.-H. Dou, T.-A. Zhang *, Y. Liu, L.-P. Niu

Fakultet za metalurgiju, Severnoistočni univerzitet, Šenjang, Kina

Apstrakt

Postupak desulfurizacije šljake koja sadrži olovo i cink je važan postupak za dobijanje olova i cinka. U ovom radu je ispitivan postupak desulfurizacije šljake sa visokim sadržajem sulfida olova i cinka postupkom uduvavanja kiseonika. Dijagrami stabilnosti Pb-Zn-Fe-S-O sistema ($Pb/(Fe+Pb+Zn)=0.176$, $Zn/(Fe+Pb+Zn)=0.56$) na različitim temperaturama su termodinamički konstruisani. Ispitivane su fizičke osobine, hemijski sastav i transformacije faze desulfurizovane šljake. Termodinamički rezultati su pokazali da olovo, cink i gvožđe mogu biti oksidovani radi dobijanja šljake sa visokim sadržajem olova i cinka. Eksperimentalni rezultati su pokazali da se sadržaj sumpora u oksidovanoj šljaki može smanjiti na manje od 1% kada se temperatura poveća na 1573K. XRD analiza kaljene šljake je pokazala da su se faze PbS i ZnS smanjile, dok su se faze cinkita i magnezijum aluminata ($Zn_xFe_{3-x}O_{4+y}$) pojavile i povećale kako se vreme reakcije povećavalo. Postupak desulfurizacije rastopljene šljake se posmatrao kao reakcija prvog reda, a aktivaciona energija je procenjena na 44,46 kJ/mol. Pod eksperimentalnim uslovima, prenos mase u gasnoj i tečnoj fazi je verovatno bio ograničavajući korak.

Ključne reči: Ruda olova i cinka; Šljaka sa visokim sadržajem sulfida olova i cinka; Desulfurizacija; Kinetika.

